Journal of Chromatography A 1688 (2023) 463704

Contents lists available at ScienceDirect

Journal of Chromatography A

journal homepage: www.elsevier.com/locate/chroma

Nine-dimensional bioprofiles of Tunisian sages (*Salvia officinalis, S. aegyptiaca* and *S. verbenaca*) by high-performance thin-layer chromatography – effect-directed analyses

Amira Reguigui[a,b], Péter G. Ott[a], András Darcsi[c], József Bakonyi[a], Mehrez Romdhane[b], Ágnes M. Móricz[a,*]

[a] Plant Protection Institute, Centre for Agricultural Research, Herman O. Str. 15, Budapest 1022, Hungary
[b] Energy, Water, Environment and Process Laboratory, (LR18ES35), National Engineering School of Gabes, University of Gabes, Gabes 6072, Tunisia
[c] Pharmaceutical Chemistry and Technology Department, National Institute of Pharmacy and Nutrition, Szabolcs Str. 33, Budapest 1135, Hungary

ARTICLE INFO

Article history:
Received 11 October 2022
Revised 5 December 2022
Accepted 5 December 2022
Available online 7 December 2022

Keywords:
High-performance thin-layer chromatography (HPTLC) – effect-directed analysis (EDA)
Salvia aegyptiaca
Salvia verbenaca
Salvia officinalis
Di- and triterpenoids

ABSTRACT

Ethyl acetate extracts of Tunisian *Salvia aegyptiaca* and *S. verbenaca* aerial parts and *S. officinalis* leaves were examined via bioanalytical profiling using high-performance thin-layer chromatography (HPTLC) combined with nine bioactivity assays, namely antibacterial (*Aliivibrio fischeri, Bacillus subtilis*, and *Rhodococcus fascians*), antifungal (*Bipolaris sorokiniana*, and *Fusarium avenaceum*), radical scavenging (DPPH•), and enzyme inhibitory (α-glucosidase, acetylcholinesterase, and lipase) ones. The screening, using toluene - ethyl acetate – methanol 6:3:0.5 (*V/V/V*) as a mobile phase, revealed five bioactive zones (**a–e**) that were analyzed by HPTLC-electrospray ionization-mass spectrometry (ESI-MS). Zones **b** and **c**, observed exclusively in *S. officinalis*, were active in all assays except α-glucosidase, and only c inhibited *F. avenaceum*. Compounds in these zones were identified by HPLC-high resolution tandem MS (LC-HRMS/MS) as rosmanol/epi-rosmanol and methyl carnosate, respectively. In the bioactive zones **a** and **e**, corosolic/maslinic acid and ursolic/oleanolic acid isomer pairs were present, which could be identified in all three *Salvia* species after their HPTLC separation using pre-chromatographic derivatization with iodine and MS detection. The triterpenes inhibited *B. subtilis* and *R. fascians* bacteria and α-glucosidase enzyme. Linoleic and linolenic acids were detected in zone **d**, which showed strong lipase inhibition in all three sage species.

1. Introduction

The association of high-performance thin-layer chromatography (HPTLC) with biological, biochemical, and microchemical assays (effect-directed analysis, EDA) is an efficient tool for the non-target screening of natural bioactive compounds in complex samples [1,2]. HPTLC-EDA ensures several benefits such as uncomplicated sample preparation, the ability to quickly analyze many samples at the same time, and the targeted identification of biologically active substances [3].

Due to the presence of active substances in medicinal plants, their bioactivity and therapeutic effects (treatment of diseases as well as improvement of health and well-being) have been exploited around the world [4]. Thus, the discovery of substances that affect living organisms has been ideally accompanied by the characterization of the individual chemical substance designated by HPTLC-EDA [5]. Furthermore, coupling HPTLC with mass spectrometry (MS) has been established as an efficient tool for the characterization process [5]. A TLC-MS interface was introduced to extract the separated substance from a solid adsorbent using an eluting solvent directed by a pump system and lead the eluate immediately into the MS [5].

Salvia aegyptiaca L., *S. verbenaca* L., and *S. officinalis* L. belong to the largest genera of medicinal and aromatic plants in the Lamiaceae family, including over 900 species in the world [6,7]. In Tunisia, ten *Salvia* species are distributed spontaneously in arid regions [6]. *Salvia* plants have been deemed as a source of natural antimicrobial, antioxidant, anti-inflammatory, neuroprotective, and anticancer agents [8–11]. It has been confirmed that several *Salvia* species (depending on their traditional uses) can ameliorate memory, quicken the senses, and treat dementia that affects memory, thinking, and behavior ('head and brain' function) as well as heal inflammations (angina, mouth, throat, bronchial asthma, and

* Corresponding author.
E-mail address: moricz.agnes@atk.hu (Á.M. Móricz).

https://doi.org/10.1016/j.chroma.2022.463704

coughs), depression, sweating, and disorders of the digestive and circulatory systems [7,12]. In addition, diterpenes (tanshinones, carnosic acid, and carnosol), triterpenes (ursolic acid and oleanolic acid), polyphenol compounds including phenolic acids (caffeic, rosmarinic, salvianolic, lithospermic, sagernic and yunnaneic acids as well as sagecoumarin), and flavonoids (luteolin, apigenin, hispidulin, kaempferol, and quercetin) have been considered as the most active constituents of sages [7,13].

Due to their therapeutic properties and richness in a vast variety of chemical compounds, *S. aegyptiaca* [14–16], *S. verbenaca* [17], and *S. officinalis* [18] have been used traditionally as herbal medicines. Yet, few studies were performed previously to bioprofile polar or nonpolar extracts of *Salvia* species, such as *S. miltiorrhiza* (roots) [19,20] or *S. officinalis* (leaf tincture or its botanical extract) [21–24], while using HPTLC-(bio)assays to confirm their bioactivity. Rosmarinic acid, lithiospermic acid and salvianolic acid B were identified as acetylcholinesterase (AChE) inhibitors and antioxidants in *S. miltiorrhiza* roots [20]. Moreover, a recent study using HPTLC hyphenations confirmed that tanshinones, triterpenoids, and phenolic acids in ethanol-water and ethyl acetate extracts from aerial parts of Tunisian *S. aegyptiaca* and *S. verbenaca* have antibacterial activities against *Aliivibrio fischeri* and *Bacillus subtilis* as well as AChE, butyrylcholinesterase (BChE), α-glucosidase, ß-glucosidase, ß-glucuronidase, tyrosinase inhibiting properties and antioxidant effects [25]. Besides, a caffeic acid derivative, as well as oleanolic acid and/or ursolic acid, have been characterized in the ethyl acetate extract of *S. verbenaca* as BChE inhibitors and antibacterials against *B. subtilis*, respectively, by high-resolution mass spectrometry [25].

This paper aimed to continue the previous study [25], using the same sage samples along with new Hungarian ones and expanded bioassays, as well as to clarify the presence of triterpenic acids. The comparison of bioprofiles of ethyl acetate extracts of Tunisian *S. aegyptiaca* and *S. verbenaca* aerial parts, as well as *S. officinalis* leaves was performed by HPTLC-EDA using nine antimicrobial, antioxidant, and enzyme inhibitory assays. In addition, profiles of *S. officinalis* from Tunisia were compared to those of Hungarian *S. officinalis* samples. For this purpose, the three sage species were screened in one hand by previously used [25] HPTLC-based assays (*Aliivibrio fischeri*, and *Bacillus subtilis* bacterial strains, the DPPH• free radical, and acetylcholinesterase and α-glucosidase enzymes), and for the first time by HPTLC combined with plant pathogenic *Rhodococcus fascians* bacterium, and *Bipolaris sorokiniana* and *Fusarium avenaceum* fungal strains, as well as lipase enzyme (lipase inhibitors reducing the efficiency of dietary fat absorption can be effective anti-obesity agents). Additionally, HPTLC-ESI-MS and HPLC-HRMS/MS were utilized for the identification of the most potent compounds.

2. Materials and methods

2.1. Materials

Ethyl acetate, toluene, methanol, acetone, sulfuric acid, ethanol, and DMSO were obtained from Reanal (Budapest, Hungary) or Molar Chemicals (Halásztelek, Hungary). Acetonitrile (LiChrosolv®, hypergrade for LC-MS) and formic acid (98–100% for LC-MS) were supplied by Merck (Darmstadt, Germany). Aluminium-chloride and vanillin were from Reanal. Fast Blue B Salt, DPPH• (1,1-diphenyl-2-picrylhydrazyl), primuline, linoleic acid, and linolenic acid were supplied by Sigma-Aldrich (Budapest, Hungary). Natural product (NP) (diphenylboryloxyethylamine, or diphenylboric acid β-ethylamino ester) reagent and MTT (3-[4,5- Dimethylthiazol-2-yl]-2,5-diphenyltetrazolium bromide), were purchased from Carl Roth (Karlsruhe, Germany). 3-Indoxylacetate, α-naphthyl acetate, 2-naphthyl-α-D-glucopyranoside, oleanolic acid (**O**), ursolic acid (**U**), corosolic acid (**C**), maslinic acid (**M**), acarbose, and orlistat were provided by BioSynth (Bratislava, Slovakia). Lipase (from porcine pancreas), acetylcholinesterase (AChE, from *Electrophorus electricus*), bovine serum albumin, and aluminum foil-backed fine particle silica gel 60 F_{254} (HPTLC, 1.05548.0001) layers were delivered by Merck. α-Glucosidase (from *Saccharomyces cerevisiae*) was obtained from NOACK Magyarország Kft. (Budapest, Hungary).

The Gram-positive *Bacillus subtilis* bacterium F1276 was a gift by József Farkas (Central Food Research Institute, Budapest, Hungary), whereas the phytopathogen *Rhodococcus fascians* bacterium (B.01608) was from NCAIM (National Collection of Agricultural and Industrial Microorganisms, Budapest, Hungary). The Gram-negative *Aliivibrio fischeri* DSM 7151 bacterial strain was supplied by Leibniz Institute DSMZ (German Collection of Microorganisms and Cell Cultures, Berlin, Germany). *Fusarium avenaceum* (Fr.) Sacc., isolate IMI 319947 was acquired from the CAB International (formerly IMI) Culture Collection (Egham, UK), while the *Bipolaris sorokiniana* (Sacc.) Shoemaker isolate H-299 was collected from barley in Hungary (NCBI GenBank accession No. MH697869).

2.2. Plant origin and sample preparation

The same collected samples of Tunisian *S. aegyptiaca* (from Bouhedma National Park, Matmata (Gabes), and Beni khedache (Medenine)) and *S. verbenaca* (from Bouhedma National Park) aerial parts according to a recently published article [25], were used also in this study (Table S1). Also, the leaf sample of Tunisian *S. officinalis* was collected in December 2020 from Gabes by Dr. Ezzeddine Saadaoui (Regional Station of the National Research Institute of Rural Engineering Water and Forests, INRGREF, Gabes, Tunisia). Another collected sample of *S. officinalis* leaves was purchased from a gardener in Menzel Elhabib (Gabes, Tunisia) between December 2020 and February 2021 (Table S1). The leaves of two Tunisian *S. officinalis* were dried (at room temperature) in the shadow and fresh air for one month. The voucher specimens of Tunisian *Salvia* samples were preserved and deposited in the herbarium of the University of Gabes. Three samples of dry leaves of *S. officinalis* were purchased from a market in Budapest, Hungary (Table S1). According to a previously published method [25], each sample was smashed and ultrasonicated in ethyl acetate (1 g/10 mL) for 15 min after vortexing for 1 min. After centrifugation (756 × g for 15 min), the ethyl acetate extracts were centrifuged at 10,000 × g for 5 min. Then, the supernatant liquid of each extract was directly transferred to a vial and stored at 4 °C until use for HPTLC application.

2.3. Standard solutions preparation

The standard solutions of ursolic and oleanolic acids were prepared at a concentration of 0.2 mg/mL in ethanol, whereas those of corosolic, maslinic, linoleic, and linolenic acids were also prepared in ethanol but at a concentration of 0.5 mg/mL.

2.4. High-performance thin-layer chromatography

HPTLC separation of ethyl acetate extract components of Tunisian or Hungarian *Salvia* samples was carried out using an improved version of a former [25] method. Ethyl acetate extracts (1.5–15 µL/band) and standard solutions (4–15 µL/band) were applied at 8-mm distance from the bottom as 5 mm bands with 9 mm distances (the first application position was 19 mm) on the HPTLC layers using an Automatic TLC Sampler ATS3 (CAMAG, Muttenz, Switzerland). The application volume of ethyl acetate extracts was adjusted according to the (bio)assay or derivatization process used. The chromatograms were developed with 9.5 mL toluene – ethyl acetate – methanol 6:3:0.5 (*V/V/V*) as a mobile

phase in an unsaturated 20 cm x 10 cm twin trough chamber (CAMAG) to a migration distance of 75 mm (from the lower edge of the plate). The chromatograms, bioautograms, and autograms were documented at Vis or under a UV lamp (at 254 or 365 nm, CAMAG) by a digital camera (Cybershot DSC-HX60, Sony, Neu-Isenburg, Germany) depending on the (bio)assay or derivatization used. The separation of triterpene isomers was performed using previously published *in situ* pre-chromatographic derivatization [26]. Briefly, 10 µL iodine solution (2% in chloroform) was applied to the band of the deposited sample, then the layer was covered with a glass sheet for 10 min and dried for 1 min by a cold air stream of a hair dryer. The development was carried out as described above. For isolation, 100 µL of ethyl acetate extract of *S. officinalis* from Menzel Elhabib-Gabes, Tunisia (**O2**) was applied as an 80-mm band and the same mobile phase was used for development. Then, each suitable zone, determined by vanillin sulfuric acid reagent using a 0.5 cm wide strip from the chromatogram, was scraped off into a syringe connected to a Nylon filter (0.22 µm, Phenomenex) and eluted with 260 µL water-methanol 1:4 (*V*/*V*). The eluates were analyzed by HPLC-HRMS/MS.

2.5. HPTLC-Effect-directed profiling

2.5.1. HPTLC-antimicrobial assays

The preparation of *B. subtilis* F1276 [27], *R. fascians* [28], and *A. fischeri* [27] cell suspensions, as well as the antibacterial bioassays, were performed as previously published. Briefly, the developed HPTLC layer was dipped into the respective cell suspension. *A. fischeri* bioautograms were directly documented (exposition times of 40–80 s) using the iBright FL1500 Imaging System (Thermo Fisher Scientific, Budapest, Hungary) to detect the bioactive compounds as dark zones against a bright bioluminescent background. *B. subtilis* and *R. fascians* bioautograms were incubated (2 h) in a humid chamber at 37 °C and 30 °C, respectively, immersed into an aqueous solution of MTT (1 mg/mL) and incubated again (30 min) to visualize antibacterial zones as bright spots on a bluish background, where the blue color indicated the reduction of the yellow MTT by metabolically active, vital cells.

The *F. avenaceum* and *B. sorokiniana* strains were used to perform the HPTLC-antifungal assays [29,30]. Briefly, the HPTLC chromatograms were immersed into the appropriate mycelium suspension and incubated for 48–72 h (vapor chamber, 21 °C) to detect antifungal compounds as zones with a lack of visible white (*F. avenaceum*) or dark gray (*B. sorokiniana*) fungal hyphae.

2.5.2. HPTLC-enzyme inhibition assays

The HPTLC-α-glucosidase [31] and HPTLC-AChE [32] inhibition assays were achieved according to previously published methods. Briefly, in the HPTLC-α-glucosidase assay, the developed chromatogram was sprayed (airbrush, Revell, Bünde, Germany) with a substrate solution (2-naphthyl-α-D-glucopyranoside), then with the α-glucosidase solution, and incubated at 37 °C (20 min). Then, the autogram was sprayed with the chromogenic reagent (Fast Blue Salt B) to reveal the bright zones that indicated the active compounds against a violet background. The positive control was acarbose. In the HPTLC-AChE assay, the developed layer was first dipped into the substrate (3-indoxyl acetate) solution, then sprayed with the enzyme solution, and after incubation (for 20 min at 37 °C and 100% humidity), the bioautogram was documented at UV 365 nm. Dark zones against a blueish-greenish fluorescent background indicated the bioactive zones. The described HPTLC-lipase assay [33] was modified. After development, the HPTLC chromatogram was dipped into the substrate solution (α-naphthyl acetate, 1 mg/mL in ethanol). The dried plate (cold air) was sprayed with the enzyme solution (0.8 mg/mL lipase and 1 mg/mL bovine serum albumin in 0.1 M, pH 7.5 phosphate buffer). After incubation for 15 min (vapor chamber, 37 °C), the bioautogram was sprayed with Fast Blue Salt B solution (1 mg/mL, in water). The positive control was orlistat. Documentation of the dried plate was performed at white light illumination to reveal lipase-inhibiting compounds as clear zones on a violet background.

2.5.3. HPTLC-DPPH• assay

The developed layer was immersed in a DPPH• solution (0.02% methanol) to detect free radical scavengers as bright yellow zones on a purple background [27].

2.6. HPTLC-derivatizations

For chemical profiling, the developed chromatograms were immersed into different derivatization reagents as follows: (1) Aluminum chloride: 50 mg $AlCl_3$ salt in 50 mL methanol, detection of fluorescent zones at UV 366 nm; (2) Primuline: 5 mg primuline in 100 mL of acetone-water 4:1 *V/V*, detection of lipophilic compounds as blue fluorescent zones at UV 366 nm; (3) Vanillin sulfuric acid: 200 mg vanillin in 50 mL ethanol and 1 mL concentrated H_2SO_4, heated at 120 °C for 5 min, detection at white light or UV 366 nm to reveal various natural substances as colorful zones; (4) NP: 0.5% methanolic NP solution, detection of phenolics as fluorescent zones at UV 366 nm.

2.7. HPTLC-MS

For the characterization of compounds in the bioactive HPTLC zones, marked with a soft pencil based on a parallel developed HPTLC-chromatogram derivatized with vanillin sulfuric acid reagent, the online combination of a binary pump (LC-20AB, Shimadzu, Kyoto, Japan), a TLC-MS Interface (with 4 and 2 mm oval elution head, CAMAG) and a single quadrupole electrospray ionization mass spectrometer (LCMS-2020, Shimadzu) were used. The elution of the marked zones was achieved using methanol (gradient grade) with a flow rate of 0.2 mL min^{-1}. To record the full scan mass spectra (*m/z* 200–1200) in the positive and negative ionization mode, N_2 was used as the nebulizer (flow rate, 1.5 L min^{-1}) and the drying gas (flow rate, 10 L min^{-1}), the interface temperature was 350 °C, the heat block temperature was 400 °C, the desolvation line temperature was 250 °C, and the detector voltage was 4.5 kV. The software LabSolutions (5.42v, Shimadzu) was used to manage the system and acquire the data.

2.8. HPLC–ESI–qTOFMS

For the exact mass determination of the bioactive *Salvia officinalis* compounds, an Agilent 1200 Series HPLC system was used with an Agilent 6520A qTOFMS (Agilent Technologies, Santa Clara, CA, USA) equipped with a dual ESI ion source operated in negative or positive ionization mode. HPLC separation was attained on a Zorbax Eclipse XDB-C18 Solvent Saver Plus (3.5 μm) reversed-phase column (75 × 3.0 mm i.d; Agilent Technologies, Santa Clara, CA, USA). The mobile phase A consisted of water/ACN/formic acid (95:5:0.1 *V/V/V*) and the mobile phase B consisted of ACN/water/formic acid (95:5:0.1, *V/V/V*). The following gradient program was applied: 0.0 min, 0% B; 10.0 min, 100% B; 12.0 min, 100% B; 12.1 min, 0% B; 3.0 min, post-run. The solvent flow rate was 0.5 mL/min and the column temperature was set to 25 °C. The injection volume was 10 µL. UV chromatograms were recorded at 254.4 nm and the spectra were acquired in the range of 190–400 nm. Nitrogen was applied as drying gas at the temperature of 325 °C at 5 L/min, the nebulizer pressure was 40 psi. Full scan mass spectra were recorded in the positive and negative ion modes in the range of m/z 25–1700. For collision-induced dissociation (CID), the collision energy varied between 10 and 40 eV. As

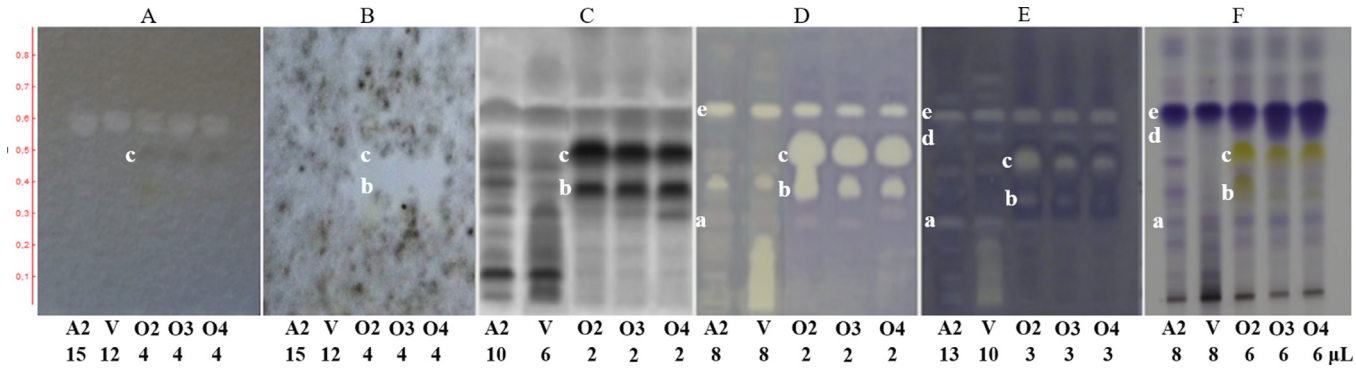

Fig. 1. HPTLC chromatogram and bioautograms of the bioactive components (**a–e**) of the Tunisian *Salvia aegyptiaca* (**A2**) and *S. verbenaca* (**V**) aerial parts and *S. officinalis* (**O2**) leaf extracts, and two Hungarian *S. officinalis* (**O3** and **O4**) leaf extracts, using *Fusarium avenaceum* (A), *Bipolaris sorokiniana* (B), *Aliivibrio fischeri* (C), *Bacillus subtilis* (D), *Rhodococcus fascians* (E), and vanillin sulfuric acid reagent (F), developed with toluene - ethyl acetate – methanol (6:3:0.5, *V/V/V*). Sources of the samples are listed in Table S1.

collision gas, high-purity nitrogen was used. The fragmentor voltage was set to 110 V and the capillary voltage was 3500 V. Product ion mass spectra were recorded in the negative ion mode in the range of m/z 50–600. Reference masses of m/z 112.985587 and 1033.988109 were used to calibrate the mass axis during analysis. Mass spectra were processed using the MassHunter Qualitative Analysis 10.0 software (Agilent).

3. Results and discussion

3.1. Bioactive substance fingerprints by HPTLC-EDA

For comparison, nine *Salvia* samples were investigated: three *S. aegyptiaca*, a *S. verbenaca*, two *S. officinalis* from Tunisia, and three *S. officinalis* from Hungary (Table S1). It was found in our previous work for the *S. aegyptiaca* and *S. verbenaca* samples [25], ethanolic extracts provided chemical profiles similar to ethyl acetate extracts in the region of bioactive semi-polar compounds, but were richer in polar matrix components (not shown). Thus, in the present study, ethyl acetate was used as an extraction solvent. The components of the three different *Salvia* species were separated with toluene - ethyl acetate - methanol 6:3:0.5 (*V/V/V*) as a mobile phase on normal phase HPTLC plates for screening the activity of individual compounds against Gram-positive (*B. subtilis* and *R. fascians*) and Gram-negative (*A. fischeri*) bacteria, fungal strains (*F. avenaceum* and *B. sorokiniana*), DPPH•, as well as acetylcholinesterase, α-glucosidase, and lipase enzymes. Compared to the previously used HPTLC method [25], the improved mobile phase without acid was found to allow the separation of the bioactive substances of the three *Salvia* species, especially under the zone **e** (Figs. 1 and S1) and it enabled skippings the neutralization of the chromatogram to make faster the whole procedure.

In the first steps of the multi-imaging discovery of the chemical- and bio-profiles of the species, ethyl acetate extracts of all 9 samples were involved (Figs. S1 and S2). We applied the ethyl acetate extracts of all the samples to do derivatization with vanillin sulfuric acid reagent (Fig. S1D and E), an antioxidative test (Fig. S1C), and antibacterial profiling against *A. fischeri* and *B. subtilis* bacteria (Fig. S2A and B). The results revealed similar HPTLC fingerprints of the samples from the same species (**A1**–**A3** and **O1**-**O5**, respectively) independently of chemical derivatization (with vanillin sulfuric acid reagent, Fig. S1D and E), *A. fischeri* and *B. subtilis* bioassays (Fig. S2A and B), and the DPPH• radical scavenging test (Fig. S1C). Therefore, for further investigations 5 samples (**A2**, **V**, **O2** from Tunisia, and **O3** and **O4** from Hungary) were selected, as representatives of the three different *Salvia* species and their geographic origins.S. officinalis

In HPTLC-EDA (bio)autograms (Figs. 1 and 2), five bioactive zones (**a**-**e**) appeared. Zone **a**, detected in all samples, showed a very weak activity against *B. subtilis* (Fig. 1D) and *R. fascians* (Fig. 1E) bacteria, and it was observed as a lipase inhibitor with low intensity (Fig. 2D). However, this zone was inactive in other assays. The low detectability could be rooted in the low abundance of the bioactive compound in the zone or its weak bio-efficiency.

Zones **b** and **c** were found exclusively in *S. officinalis* extracts and exhibited a characteristic antifungal effect against *B. sorokiniana* (Fig. 1B) and an antibacterial effect against *A. fischeri, B. subtilis*, and *R. fascians* (Fig. 1C–E); whereas only zone **c** inhibited *F. avenaceum* (Fig. 1A). Further, both zones showed strong antioxidant activity (Fig. 2A) and inhibited AChE (Fig. 2C) and lipase (Fig. 2D) enzymes.

Zones **d** and **e** were observed in all extracts. Zone **d** displayed weak activity against *R. fascians* (Fig. 1E) and strong lipase inhibition (Fig. 2D).

The intensely visible zone **e** exhibited a characteristic antibacterial effect against *B. subtilis* and *R. fascians* bacteria (Fig. 1D and E), whereas low α-glucosidase inhibitory activities (Fig. 2B).

3.2. Characterization of bioactive triterpenoids

Bioactive zones **a** and **e** were detectable as violet spots after derivatization with the vanillin sulfuric acid reagent with low and high intensities, respectively (Fig. 2H). Performing an HPTLC-ESI-MS analysis, compounds in these zones gave characteristic mass signals in negative ionization mode at *m/z* 471 $[M-H]^-$ and *m/z* 455 $[M-H]^-$, respectively. Based on these data, triterpenoids were expected as the presented compounds, notably corosolic acid (**C**) and/or maslinic acid (**M**) in zone a, as well as ursolic acid (**U**) and/or oleanolic acid (**O**) in zone **e**. The chemical structures of the two isomer pairs are very similar, differing only in the position of one methyl group (Fig. 3), thus their separation can be achieved by reversed-phase chromatography or after pre-chromatographic derivatization [26]. Applying individual standards (**U**, **O**, **C**, and **M**) and the developed HPTLC method, the co-elution of the isomers was observed at the hR_F of **a** and **e**, respectively (Fig. 4). Furthermore, all four could be responsible for the α-glucosidase (Fig. 4B) and anti-*Bacillus* [26] effect. To clarify whether the predicted triterpenes are present in the extracts, their separation was implemented by pre-chromatographic derivatization with iodine and the same mobile phase as described above (Fig. 4D). It was obvious that **U** and **O** are ingredients of the representatives of all three *Salvia* species (**A2**, **V**, and **O2**). An HPTLC-ESI-MS analysis of the chromatographic spots in the track of the samples at the R_F of the respective triterpenes (Fig. 5) and thus at the R_F of **C** and **M** proved

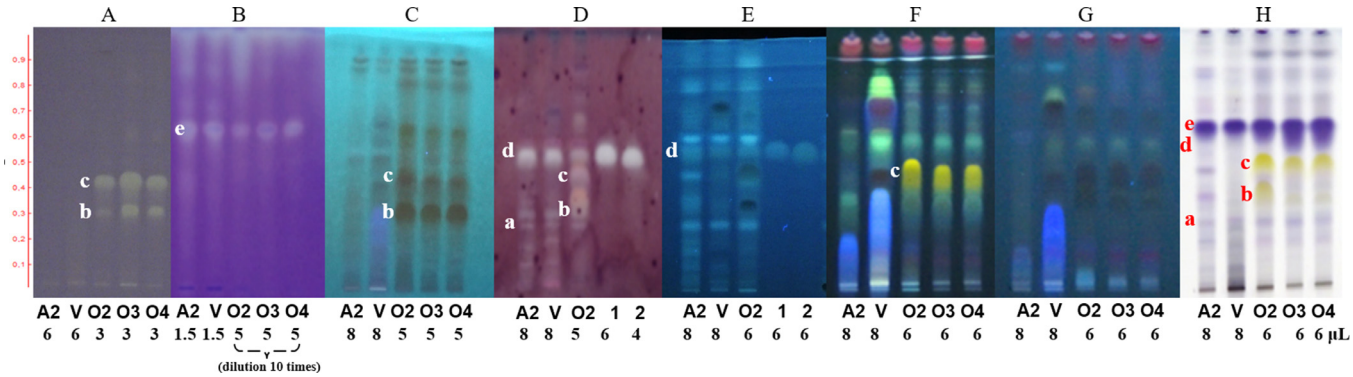

Fig. 2. HPTLC profiles of bioactive components (**a**-**e**) of *Salvia* extracts (**A2**, **V**, and **O2**-**O4**, assignments as in Fig. 1 and Table S1), developed with toluene - ethyl acetate – methanol (6:3:0.5, *V/V/V*) after DPPH• radical scavenging test (A), and α-glucosidase (B), acetylcholinesterase (C), and lipase (D) enzyme inhibition assays, as well as derivatization with primuline (E), natural product (F), aluminium-chloride (G) and vanillin sulfuric acid (H) reagents, detected at white light illumination (A, B, D, and H), or at UV 365 nm (C, and E-G). **1** and **2** are linoleic and linolenic acids, respectively.

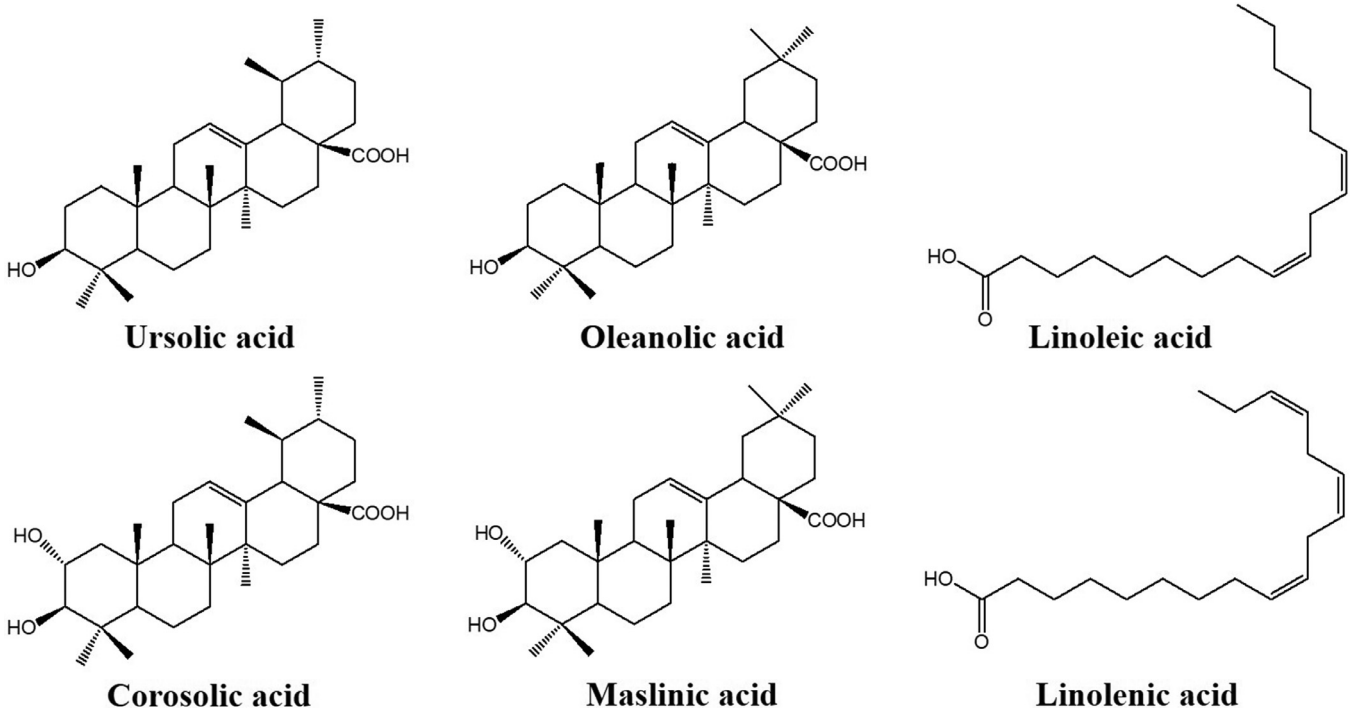

Fig. 3. Chemical structures of the identified bioactive compounds of Tunisian *Salvia* species

the presence of both **C** and **M** in the three species (Fig. 5C and D). *Salvia* extracts were rich in **U** and **O**, but **C** and **M** had low abundance, therefore, the latter two, despite their effectiveness, could not reach the minimal effective concentration in the samples in all assays (e.g. Fig. 4B). Based on literature data, **U** and **O** triterpenes have been described in *Salvia* species. They were previously isolated e.g. from ethanolic extract of *S. cerino-pruinosa* aerial and root parts [34], methanolic extracts of *S. pomifera* and *S. fruticosa* aerial parts [35], methanolic extract of cultivated *S. officinalis* aerial part [36], and aerial parts of *S. aegyptiaca* [37]. More recently, the presence of **U** and/or **O** (they were not separated by HPTLC) in the ethyl acetate extract of the *S. verbenaca* aerial part was reported [25]. In addition, the identification of **M** and **C** in several *Salvia* species, such as **M** in *S. lachnostachys* leaves [38], *S. multicaulis* aerial parts [39], and flowers of *S. miltiorrhiza* [40], as well as **C** in leaf extract of *S. officinalis* [41], aerial parts of *S. mellifera* [42] and *S. plebeia* [43], flowers of *S. miltiorrhiza* [40], and *S. chinensis* [44] have been published. Terpenoids, including **U** and **O**, are potential AChE inhibitors and thus possible agents in the therapy of Alzheimer's disease [45]. However, in our HPTLC-AChE assay, none of the four identified triterpenes showed activity. The α-glucosidase inhibition of **U**, **O**, **C**, and **M** has been reported [46], and with it the promise to cure diabetes. The strong inhibition effect of **U** and **O** on this enzyme has been confirmed, using the methanolic extract of *S. africana-lutea* [47] and 14 Turkish *Salvia* species as sources against diabetes [48]. An anti-obesity property [49] and a hypoglycemic effect of **O** (by stimulating serum insulin, inhibition of gluconeogenesis, and lowering accelerated blood glucose in parallel with reduction of body weight after its administration to diabetic mice) [50] have been demonstrated. Also, the antidiabetic effect of **C** on animals and humans has been described [51]. The antibacterial activity of **U** and **O** from the acetone extract of *S. officinalis* leaves has been reported against Gram-positive bacteria, along with their inefficiency against Gram-negative ones [52]. **U** in *Salvia* extracts has been characterized owing to its strong antibacterial activity (about 175 times more active) against Gram-positive bacteria compared to **O** [53]. The anti-*Bacillus* activity of **U**, **O**, **C**, and **M** has been shown by an HPTLC-based assay after

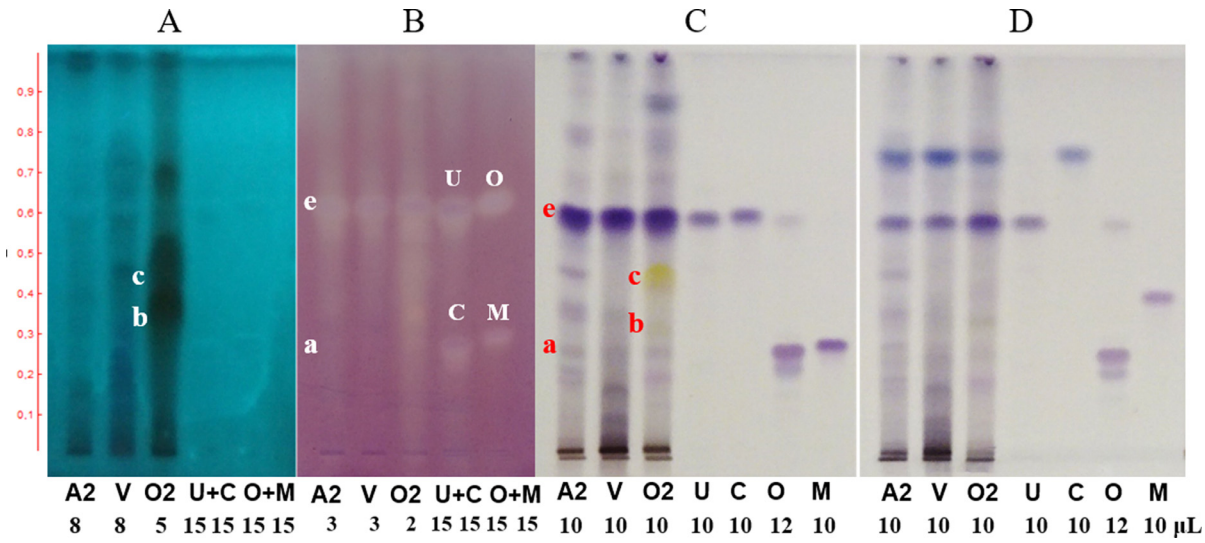

Fig. 4. HPTLC autograms after acetylcholinesterase (A) and α-glucosidase (B) enzyme inhibition assays as well as HPTLC chromatograms after derivatization with vanillin sulfuric acid (C and D) of Tunisian *Salvia* extracts (**A2**, **V**, and **O2**, assignments as in Fig. 1 and Table S1), and the individual standard ursolic (**U**), oleanolic (**O**), corosolic (**C**), and maslinic (**M**) acids, developed with toluene - ethyl acetate – methanol (6:3:0.5, *V/V/V*), and detected at UV 365 nm (A) or white light illumination (B-D). Separation of the isomeric triterpene pairs was achieved using pre-chromatographic derivatization with iodine (D).

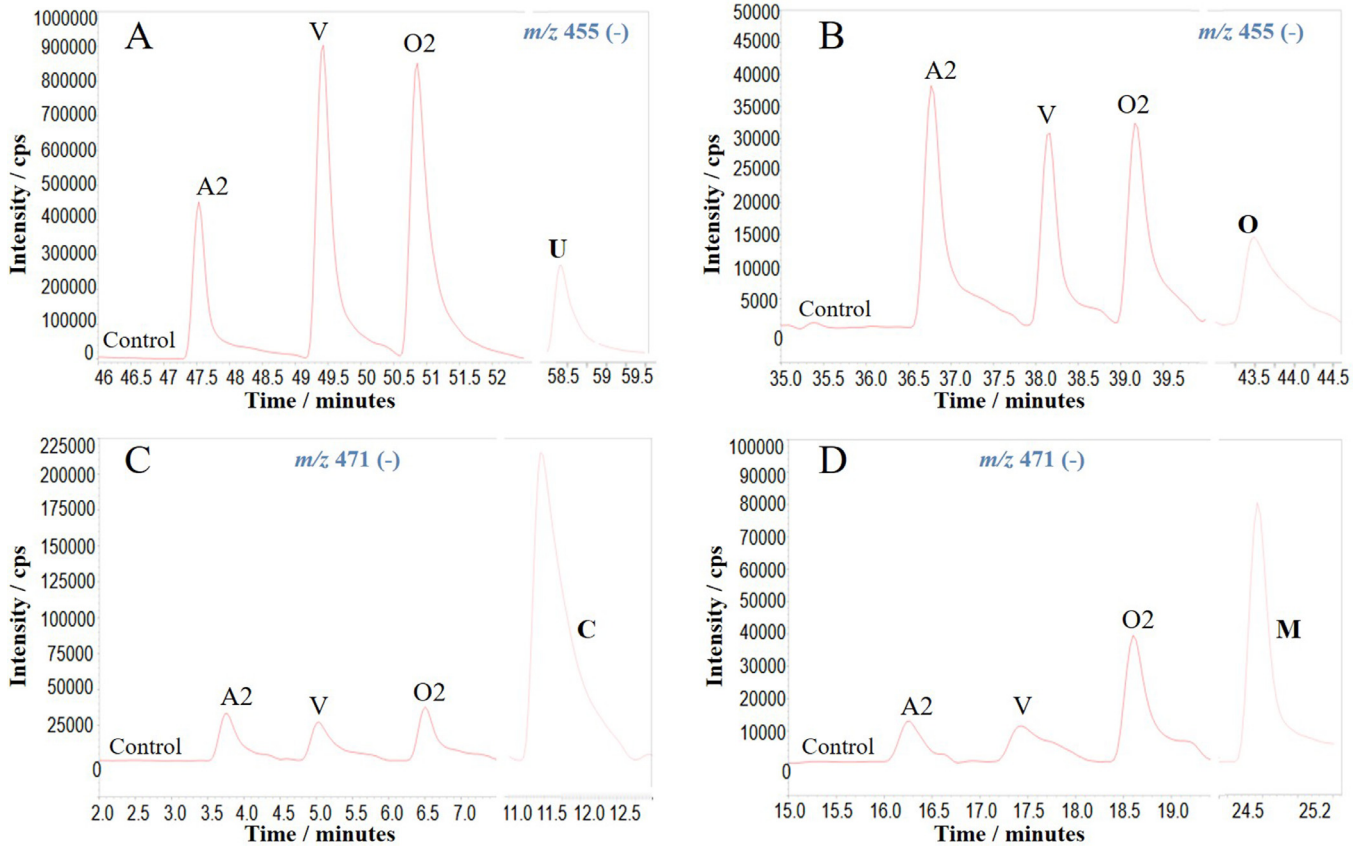

Fig. 5. HPTLC-ESI-MS detection (via extracted ion chronograms at *m/z* 471 or *m/z* 455) of ursolic acid (**U**, A), oleanolic acid (**O**, B) corosolic acid (**C**, C), and maslinic acid (**M**, D) in Tunisian *Salvia aegyptiaca* (**A2**), *S. verbenaca* (**V**), and *S. officinalis* (**O2**) ethyl acetate extracts separated with toluene - ethyl acetate – methanol, (6:3:0.5, (*V/V/V*) after pre-chromatographic derivatization with iodine, using elution-head based interface and negative ionization mode.

Table 1
Assignment of LC-HRMS/MS signals of isolated compounds in zones **b** and **c** of the ethyl acetate extract of the *S. officinalis* leaves collected from Menzel Elhabib-Gabes, Tunisia (**O2**).

Zone	Modes	Observed *m/z*	Theoretical *m/z*	Molecular formula	Mass error (ppm)	Assignment	identified compounds
b	ESI-MS	345.17050	345.16965	$C_{20}H_{25}O_5^-$	2.48	$[M-H]^-$	Rosmanol/Epi-rosmanol
	ESI-MS	691.34892	691.34767	$C_{40}H_{51}O_{10}^-$	1.80	$[2M-H]^-$	
	ESI+MS	347.18530	347.18530	$C_{20}H_{27}O_5^+$	0.01	$[M+H]^+$	
	ESI+MS	369.16682	369.16725	$C_{20}H_{26}O_5Na^+$	1.16	$[M+Na]^+$	
	ESI+MS	301.17972	301.17982	$C_{19}H_{25}O_3^+$	0.34	$[M-CO_2H]^+$	
	ESI+MS	715.34486	715.34527	$C_{40}H_{52}O_{10}Na^+$	0.57	$[2M+Na]^+$	
	MS2[345]	301.18062	301.17982	$C_{19}H_{25}O_3^-$	2.65	$[M-CO_2H]^-$	
	MS2[345]	283.17031	283.16926	$C_{19}H_{23}O_2^-$	3.72	$[M-CO_2H-H_2O]^-$	
c	ESI-MS	345.20801	345.20604	$C_{21}H_{29}O_4^-$	5.73	$[M-H]^-$	Methyl carnosate
	ESI-MS	713.40577	713.40239	$C_{42}H_{58}O_8Na^-$	4.74	$[2M-2H+Na]^-$	
	ESI-MS	1081.60153	1081.59874	$C_{63}H_{87}O_{12}Na_2^-$	2.57	$[3M-3H+Na_2]^-$	
	ESI+MS	347.22096	347.22169	$C_{21}H_{31}O_4^+$	2.09	$[M+H]^+$	
	ESI+MS	369.20326	369.20363	$C_{21}H_{30}O_4Na^+$	1.01	$[M+Na]^+$	
	ESI+MS	301.22001	301.21621	$C_{20}H_{29}O_2^+$	12.67	$[M-CO_2H]^+$	
	ESI+MS	715.42985	715.41804	$C_{42}H_{60}O_8Na^+$	16.52	$[2M+Na]^+$	
	MS2[345]	301.21653	301.21621	$C_{20}H_{29}O_2^-$	1.08	$[M-CO_2H]^-$	
	MS2[345]	286.19292	286.19273	$C_{19}H_{26}O_2^-$	0.66	$[M-CO_2H-CH_3]^-$	

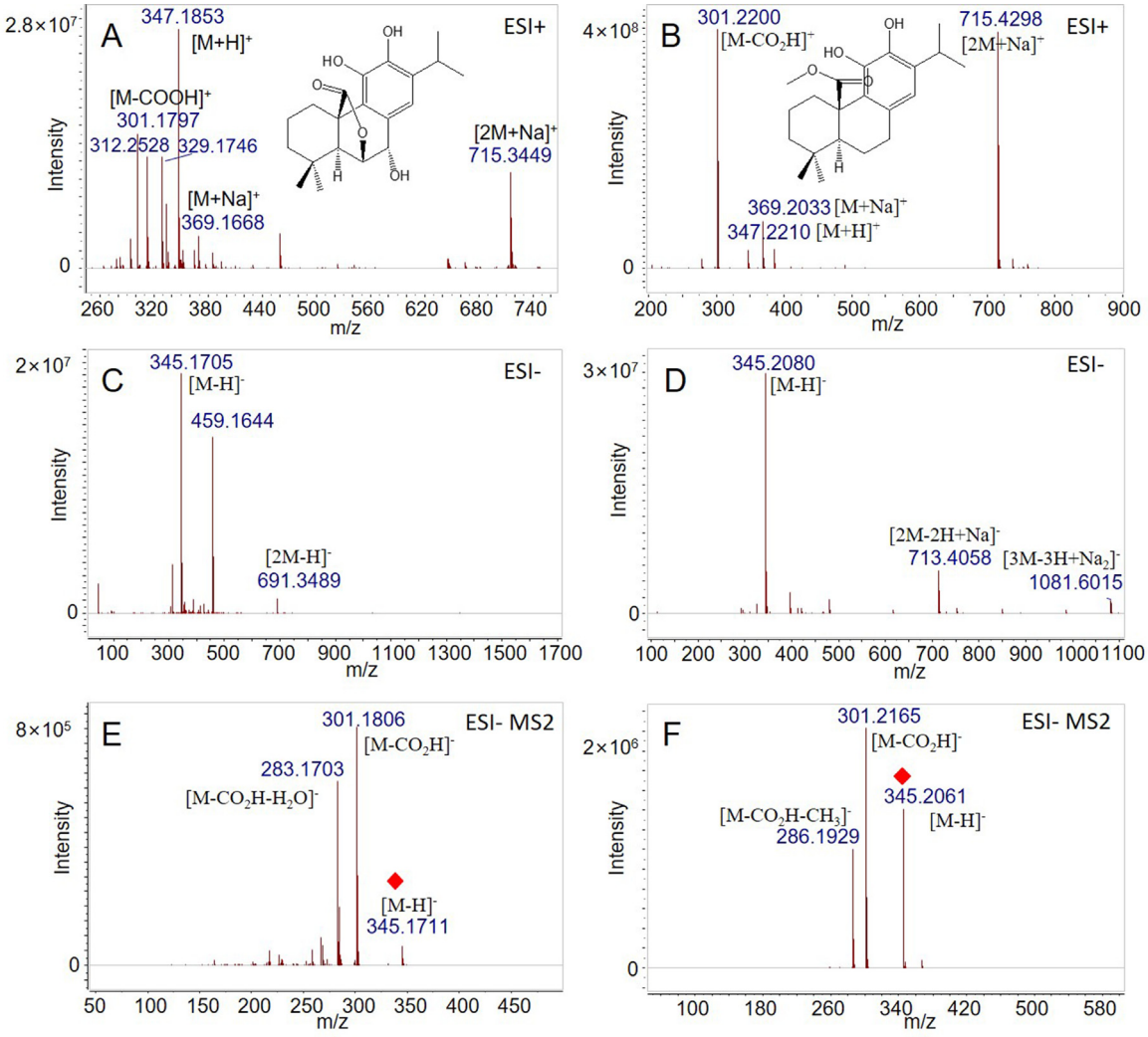

Fig. 6. HPLC-ESI-HRMS spectra in positive (A and B) and negative (C and D) ionization modes, of zones **b** (A and C) and **c** (B and D) of the Tunisian *S. officinalis* (**O2**) ethyl acetate extract developed with toluene - ethyl acetate – methanol, (6:3:0.5, (*V/V/V*), and HRMS/MS spectra of the deprotonated molecules (E and F, respectively).

the separation of the four triterpenoids using pre-chromatographic derivatization with iodine [26]. The α-glucosidase and *B. subtilis* inhibition of the HPTLC zone of **U**/**O** has already been confirmed in ethyl acetate extracts of Tunisian *S. verbenaca* and *S. aegyptiaca* aerial parts as well [25].

3.3. Identification of the main lipase inhibitors

The mass spectrometric evaluation of zone **d** by HPTLC-MS in the negative ionization mode resulted in the detection of characteristic mass signals at *m/z* 279, and *m/z* 277, which were assigned

the deprotonated molecules $[M-H]^-$ of compounds that were tentatively identified as linoleic and linolenic acids, respectively. The chromatographic behavior, the detectability with primuline (suitable for lipophilic compounds) and vanillin sulfuric acid reagents, and lipase inhibitory effects of zone **d** were the same as those of linoleic and linolenic acids, which confirmed the identification (Figs. 2 and 3).

According to the literature, fatty acids like linoleic and linolenic acids have been identified in the petroleum ether extract of *S. bicolor* aerial part [54], and linoleic acid in the dichloromethane extract of *S. officinalis* leaves [55]. The lipase inhibitory activity of the methanolic extract from *S. officinalis* leaves [56], as well as that of linoleic acid, has been previously demonstrated [57].

3.4. Identification of main bioactive compounds of S. officinalis

The preliminary HPTLC-MS analysis of zones **b** and **c** showed the same mass signals at *m/z* 345 $[M-H]^-$ and *m/z* 369 $[M+Na]^+$. To identify these compounds, they were isolated from **O2** and characterized by HPLC-HRMS/MS. Their accurate mass spectra were recorded in the positive and negative ionization modes (+ure 6, Table 1). For zone **b**, the mass signals in positive ionization (Fig. 6A) at *m/z* 347.1853 $[M+H]^+$, *m/z* 301.1797 $[M-COOH]^+$, *m/z* 369.1668 $[M+Na]^+$, and *m/z* 715.3449 $[2M+Na]^+$, whereas in negative ionization at *m/z* 345.1705 $[M-H]^-$, *m/z* 691.3489 $[2M-H]^-$ (ESI-, Fig. 6C) were assigned to rosmanol ($C_{20}H_{26}O_5$, a diterpene). The fragmentation patterns of the deprotonated molecules with *m/z* 301.1806 $[M-CO_2H]^-$ and *m/z* 283.1703 $[M-CO_2H-H_2O]^-$ (ESI-MS2, Fig. 6E) were in harmony with the literature data [58], thus confirming the identity of rosmanol or its isomer epi-rosmanol. For zone **c**, the mass signals in positive ionization at *m/z* 301.2200 $[M-CO_2H]^+$, *m/z* 347.2210 $[M+H]^+$, *m/z* 369.2033 $[M+Na]^+$, and *m/z* 715.4298 $[2M+Na]^+$ (Fig. 6B), in negative ionization at *m/z* 345.2080 $[M-H]^-$, *m/z* 713.4058 $[2M-2H+Na]^-$, *m/z* 1081.6015 $[3M-3H+Na_2]^-$ (ESI-, Fig. 6D), and the fragments of the deprotonated ion at *m/z* 301.2165 $[M-CO_2H]^-$ and *m/z* 286.1929 $[M-CO_2H-CH_3]^-$ (ESI- MS2, Fig. 6F) were assigned, according to literature data [59], to methyl carnosate ($C_{21}H_{30}O_4$, diterpene). Comparing the HPTLC-MS and the HPLC-HRMS/MS results, the identity of the compounds was not modified throughout the isolation step. Both rosmanol and methyl carnosate, in zones **b** and **c** respectively, were detectable by the HPTLC-vanillin sulfuric acid derivatization (Figs. 2H and S2) in all *S. officinalis* ethyl acetate extracts as yellow zones and this was confirmative of the presence of terpenoids. In addition, zone **c** (and not zone **b**) was detectable as a yellow zone after derivatization with natural product reagent (Fig. 2F), however, it was not observed after derivatization with aluminum-chloride (Fig. 2G), indicating that phenolics, but not flavonoids, were found in *S. officinalis* extracts.

There are several studies reported to support the bioactivity of the two identified diterpenes. Rosmanol and epi-rosmanol have been detected in *S. officinalis* leaves [60], in the methanolic extract of *S. fruticosa* and *S. pomifera* dried aerial parts [35] as major phenolic diterpene components, and in *S. chamelaeagnea* methanolic extract as a strong antioxidant [61]. Furthermore, rosmanol and epi-rosmanol exhibited anti-protozoal, cytotoxic [62], and antibacterial [63,64] effects as well. According to literature data, methyl carnosate has been determined as a major phenolic diterpene in aerial parts of *S. officinalis* [65,66], Tunisian *S. aegyptiaca* [67,68], and *S. verbenaca* [69]; however, in the latter ones we could not detect it. Its strong antioxidant activity [70] as well as the antibacterial effect against *Bacillus cereus* [66] have been published. Moreover, the antioxidative activity of the phenolic diterpenes of *S. officinalis* has been proven [71], and due to its high antioxidant capacity and antibacterial activity, the *S. officinalis* extract was used as a natural preservative in meat [72]. Additionally, the antibacterial activity against methicillin-sensitive and -resistant *Staphylococcus aureus* and *Enterococcus faecalis* [73], and the cytotoxic effect [74] of methyl carnosate have been published.

4. Conclusion

The bioprofiles of ethyl acetate extracts from three *Salvia* species (*S. aegyptiaca, S. verbenaca*, and *S. officinalis*) were studied by HPTLC-EDA using Gram-positive *B. subtilis* and *R. fascians*, Gram-negative *A. fischeri* bacterial strains, *F. avenaceum* and *B. sorokiniana* fungal strains, DPPH• stable radical, and acetylcholinesterase, lipase, and α-glucosidase enzymes. This nine-dimensional, comprehensive bioprofile revealed four antibacterial triterpenic acids (corosolic, maslinic, ursolic, and oleanolic acid) and two fatty acids (linoleic and linolenic acid) with anti-lipase activity, which were identified by HPTLC-UV/Vis/FLD-MS analysis using standards. Furthermore, multi-potent phenolic diterpenes (rosmanol/epi-rosmanol and methyl carnosate) were tentatively identified after isolation by HPLC-HRMS/MS. This HPTLC-based screening system, comprising antibacterial, antifungal, antioxidant, and enzyme-inhibitory assays, was found to be a powerful, straightforward platform for high-throughput fishing of compounds against infectious or enzyme-related diseases, so very useful in drug discovery.

Declaration of Competing Interest

The authors declare that they have no known competing financial interests or personal relationships that could have appeared to influence the work reported in this paper. The authors declare no conflict of interest.

CRediT authorship contribution statement

Amira Reguigui: Investigation, Writing – original draft. **Péter G. Ott:** Methodology, Resources, Writing – review & editing. **András Darcsi:** Investigation. **József Bakonyi:** Methodology, Resources, Writing – review & editing. **Mehrez Romdhane:** Supervision. **Ágnes M. Móricz:** Conceptualization, Supervision, Methodology, Resources, Investigation, Formal analysis, Writing – original draft, Writing – review & editing.

Data availability

No data was used for the research described in the article.

Acknowledgments

Thanks are owed to the University of Gabes supported by the Ministry of Higher Education and Scientific Research of Tunisia for the alternating scholarship (2020-BALT-1354) that allowed A. R. to stay at the Plant Protection Institute, Centre for Agricultural Research, Budapest, Hungary. The authors thank Dr. Mustapha Gorai and Dr. Ezzeddine Saadaoui for collecting Tunisian *S. aegyptiaca* and *S. verbenaca* aerial parts as well as *S. officinalis* leaf samples, respectively. This work was partially funded by the National Research, Development and Innovation Office of Hungary (NKFIH SNN139496).

References

[1] G.E. Morlock, W. Schwack, Hyphenations in planar chromatography, J. Chromatogr. A 1217 (2010) 6600–6609.

[2] Á.M. Móricz, P.G. Ott, T.T. Häbe, A. Darcsi, A. Böszörményi, Á. Alberti, D. Krüzselyi, P. Csontos, S. Béni, G.E. Morlock, Effect-directed discovery of bioactive compounds followed by highly targeted characterization, isolation and identification, exemplarily shown for *Solidago virgaurea*, Anal. Chem. 88 (2016) 8202–8209.

[3] G.E. Morlock, Bioassays | effects-detection in chromatography, in: P.J. Worsfold, C. Poole, A. Townshend, M. Miro (Eds.), Reference Module in Encyclopedia of Analytical Science, third ed., Elsevier, 2018, pp. 261–270, doi:10.1016/B978-0-12-409547-2.13959-9.

[4] S.G. Bhat, Medicinal plants and its pharmacological values, in: H.A. El-Shemy (Ed.), Natural Medicinal Plants, IntechOpen, London, UK, 2021.

[5] Á.M. Móricz, P.G. Ott, Screening and characterization of antimicrobial components of natural products using planar chromatography coupled with direct bioautography, spectroscopy and mass spectrometry: a review, Curr. Org. Chem. 21 (2017) 1861–1874.

[6] E. Le Floc'h, L. Boulos, E. Vela, Catalogue Synonymique Commenté de la Flore de Tunisie, Ministère de L'environnement et Du Développement Durable, Banque Nationale Des Gènes, Tunis, Tunisie, 2010.

[7] A.L. Lopresti, *Salvia* (sage): a review of its potential cognitive-enhancing and protective effects, Drugs R D 17 (2017) 53–64.

[8] M. Bonesi, M.R. Loizzo, R. Acquaviva, G.A. Malfa, F. Aiello, R. Tundis, Anti-inflammatory and antioxidant agents from *Salvia* genus (Lamiaceae): An assessment of the current state of knowledge, AntiInflamm. AntiAllergy Agents Med. Chem. 16 (2017) 70–86.

[9] D.C. Hao, G.B. Ge, P.G. Xiao, Anticancer drug targets of *Salvia* phytometabolites: chemistry, biology and omics, Curr. Drug Targets 19 (2018) 1–20.

[10] A. Ververis, G. Savvidou, K. Ioannou, P. Nicolaou, K. Christodoulou, M. Plioukas, Greek sage exhibits neuroprotective activity against amyloid beta-induced toxicity, Evid. Based Complement. Altern. Med. 2020 (2020) 2975284.

[11] A.F. Afonso, O.R. Pereira, S.M. Cardoso, *Salvia* species as nutraceuticals: Focus on antioxidant, antidiabetic and anti-obesity properties, App. Sci. 11 (2021) 9365 (Switzerland).

[12] E.K. Perry, A.T. Pickering, W.W. Wang, P.J. Houghton, N.S.L. Perry, Medicinal plants and Alzheimer's disease: from ethnobotany to phytotherapy, J. Pharm. Pharmacol. 51 (1999) 527–534.

[13] Y. Lu, L.Y Foo, Polyphenolics of *Salvia*—a review, Phytochemistry 59 (2002) 117–140.

[14] M.A. Al Yahya, I.A. Al Meshal, J.S. Mossa, A.A. Al Badr, M. Tariq, *Salvia aegyptiaca* Linn, in: Saudi Plants: Phytochemical and biological approach, King Abdul Aziz City for Science and Technology, Riyadh Saudi Arabia, 1990, pp. 365–367.

[15] A. Rizk, G. El-Ghazaly, *Salvia aegyptiaca* L, in: Medicinal and Poisonous Plants Of Qatar, Science and Applied Research Centre, University of Qatar, King Print of Richmond, 1995, pp. 140–141.

[16] S.A. Ghazanfar, *Salvia aegyptiaca*. L, Handbook of Arabian Medicinal Plants, CRC Press, Boca Raton, 1999.

[17] A. Khouchlaa, A. Et-Touys, F. Lakhdar, F.E. Laasri, A. El Yahyaoui El Idrissi, F. Zaakour, Ethnomedicinal use, phytochemistry, pharmacology, and toxicology of *Salvia verbenaca* L. : a review, Biointerface Res. Appl. Chem. 12 (2022) 1437–1469.

[18] M. Hamidpour, R. Hamidpour, S. Hamidpour, M. Shahlari, Chemistry, pharmacology, and medicinal property of sage (*Salvia*) to prevent and cure illnesses such as obesity, diabetes, depression, dementia, lupus, autism, heart disease, and cancer, J. Tradit. Complement. Med. 4 (2014) 82–88.

[19] M. Jamshidi-Aidji, G.E. Morlock, From bioprofiling and characterization to bioquantification of natural antibiotics by direct bioautography linked to high-resolution mass spectrometry: Exemplarily shown for *Salvia miltiorrhiza* root, Anal. Chem. 88 (2016) 10979–10986.

[20] E. Azadniya, G.E. Morlock, Bioprofiling of *Salvia miltiorrhiza* via planar chromatography linked to (bio)assays, high resolution mass spectrometry and nuclear magnetic resonance spectroscopy, J. Chromatogr. A 1533 (2018) 180–192.

[21] W. Jesionek, E.M. Grzelak, B. Majer-Dziedzi, I.M. Choma, Thin-layer chromatography — direct bioautography for the screening of antimicrobial properties of plant extracts, J. Planar Chromatogr. Mod. TLC 26 (2013) 109–113.

[22] M. Jamshidi-Aidji, G.E. Morlock, Bioprofiling of unknown antibiotics in herbal extracts: development of a streamlined direct bioautography using *Bacillus subtilis* linked to mass spectrometry, J. Chromatogr. A 1420 (2015) 110–118.

[23] W. Jesionek, B. Majer-Dziedzic, G. Horváth, Á.M. Móricz, I.M. Choma, Screening of antibacterial compounds in *Salvia officinalis* L. tincture using thin-layer chromatography—direct bioautography and liquid chromatography—tandem mass spectrometry techniques, J. Planar Chromatogr. Mod. TLC 30 (2017) 357–362.

[24] S. Krüger, L. Hüsken, R. Fornasari, I. Scainelli, G.E. Morlock, Effect-directed fingerprints of 77 botanical extracts via a generic high-performance thin-layer chromatography method combined with assays and mass spectrometry, J. Chromatogr. A 1529 (2017) 93–106.

[25] A. Reguigui, J. Heil, M. Gorai, M. Mabrouk, M. Romdhane, G.E. Morlock, Profile comparison and valorization of Tunisian *Salvia aegyptiaca* and *S. verbenaca* aerial part extracts via hyphenated high-performance thin-layer chromatography, J. Chromatogr. A 1673 (2022) 463057.

[26] Á.M. Móricz, P.G. Ott, Separation and detection of apricot leaf triterpenes by high-performance thin-layer chromatography combined with direct bioautography and mass spectrometry, J. Chromatogr. A 1675 (2022) 463167.

[27] Á.M. Móricz, T.T. Häbe, P.G. Ott, G.E. Morlock, Comparison of high-performance thin-layer with overpressured layer chromatography combined with direct bioautography and direct analysis in real time mass spectrometry for tansy root, J. Chromatogr. A 1603 (2019) 355–360.

[28] M. Baglyas, P.G. Ott, Z. Garádi, V. Glavnik, S. Béni, I. Vovk, Á.M. Móricz, High-performance thin-layer chromatography – antibacterial assay first reveals bioactive clerodane diterpenes in giant goldenrod (*Solidago gigantea* Ait.), J. Chromatogr. A 1677 (2022) 463308.

[29] Á.M. Móricz, D. Krüzselyi, P.G. Ott, Z. Garádi, S. Béni, G.E. Morlock, J. Bakonyi, Bioactive clerodane diterpenes of giant goldenrod (*Solidago gigantea* Ait.) root extract, J. Chromatogr. A 1635 (2021) 461727.

[30] D. Krüzselyi, J. Bakonyi, P.G. Ott, A. Darcsi, P. Csontos, G.E. Morlock, Á.M. Móricz, Goldenrod root compounds active against crop pathogenic fungi, J. Agric. Food Chem. 69 (2021) 12686–12694.

[31] Á.M. Móricz, M. Jamshidi-Aidji, D. Krüzselyi, A. Darcsi, A. Böszörményi, P. Csontos, S. Béni, P.G. Ott, G.E. Morlock, Distinction and valorization of 30 root extracts of five goldenrod (*Solidago*) species, J. Chromatogr. A 1611 (2020) 460602.

[32] Á.M. Móricz, D. Krüzselyi, V. Lapat, P.G. Ott, Acetylcholinesterase inhibitors in the giant goldenrod root, J. Chromatogr. B 1185 (2021) 123004.

[33] A.M.S. Hassan, TLC bioautographic method for detecting lipase inhibitors, Phytochem. Anal. 23 (2012) 405–407.

[34] A. Ertas, H. Cakirca, I. Yener, M. Akdeniz, M. Firat, G. Topcu, U. Kolak, Bioguided isolation of secondary metabolites from *Salvia cerino-pruinosa* rech. F. var. *cerino-pruinosa*, Rec. Nat. Prod. 15 (2021) 585–592.

[35] A. Koutsoulas, M. Čarnecká, J. Slanina, J. Tóth, I. Slaninová, Characterization of phenolic compounds and antiproliferative effects of *Salvia pomifera* and *Salvia fruticosa* extracts, Molecules 24 (2019) 2921.

[36] H. Abdollahi-Ghehi, A. Sonboli, S.N. Ebrahimi, M.A. Esmaeili, M.H. Mirjalili, Triterpenic acid content and cytotoxicity of some *Salvia* species from Iran, Nat. Prod. Commun. 14 (2019) 1–8.

[37] M. Bruno, R. Ciriminna, H.S. Al-Easa, A.F.M. Rizk, Triterpenoids from *Salvia aegyptiaca*, Fitoterapia 64 (1993) 275–276.

[38] C.S. Oliveira, C.J. Alvarez, M.R.P. Cabral, M.H. Sarragiotto, M.J. Salvador, M.É.A. Stefanello, Three new diterpenoids from the leaves of *Salvia lachnostachys*, Nat. Prod. Res. (2022) in press.

[39] L.M. Barhoumi, H.I. Al-Jaber, M.H.A. Zarga, A new diterpene and other constituents of *Salvia multicaulis* from Jordan, Nat. Prod. Res. (2021) 1–8.

[40] P. Liu, P. Hu, R.X. Deng, R. Li, L. Yang, W.P. Yin, Triterpenoids from the flowers of *Salvia miltiorrhiza*, Helv. Chim. Acta 94 (2011) 136–141.

[41] A.R. Velamuri, Y. Sharma, J. Fagan, J. Schaefer, C.R. Velamuri, Application of UHPLC-ESI-QTOF-MS in phytochemical profiling of sage (*Salvia officinalis*) and rosemary (*Rosmarinus officinalis*), Planta Med. 7 (2020) 133–144.

[42] Z. Ali, S. Radhakrishnan, B. Avula, A.G. Chittiboyina, J. Li, C. Wu, I.A. Khan, Eupatorin 3'-*O*-glucopyranoside, a trimethoxyflavonoid glucoside from the aerial parts of *Salvia mellifera*, Nat. Prod. Res. (2021) 1–8.

[43] S.J. Lee, H.J. Jang, Y. Kim, H.M. Oh, S. Lee, K. Jung, Y.H. Kim, W.S. Lee, S.W. Lee, M.C. Rho, Inhibitory effects of IL-6-induced STAT3 activation of bio-active compounds derived from *Salvia plebeia* R.Br, Process. Biochem. 51 (2016) 2222–2229.

[44] Q. Jiang, S. Zou, Determination of five triterpenic acids from *Salvia chinensis* of different parts by RP-HPLC-PDA, Zhongguo Zhong Yao Za Zhi 39 (2014) 4379–4382.

[45] K.Y. Yoo, S.Y. Park, Terpenoids as potential anti-Alzheimer's disease therapeutics, Molecules 17 (2012) 3524–3538.

[46] H. Du, H. Li, P. Wu, C. Wang, J. Xue, X. Wei, α-Glucosidase inhibitory pentacyclic triterpenoids from the leaves of *Cleistocalyx conspersipunctatus*, Pyhtochem. Lett. 41 (2021) 109–113.

[47] N.G.E.R. Etsassala, J.A. Badmus, T.T. Waryo, J.L. Marnewick, C.N. Cupido, A.A. Hussein, E.I. Iwuoha, Alpha-glucosidase and alpha-amylase inhibitory activities of novel abietane diterpenes from *Salvia africana-lutea*, Antioxidants 8 (2019) 421 (Basel, Switzerland).

[48] Z. Kalaycıoğlu, S. Uzaşçı, T. Dirmenci, F.B. Erim, α-Glucosidase enzyme inhibitory effects and ursolic and oleanolic acid contents of fourteen Anatolian *Salvia* species, J. Pharm. Biomed. Anal. 155 (2018) 284–287.

[49] Y. Li, J. Wang, T. Gu, J. Yamahara, Y. Li, Oleanolic acid supplement attenuates liquid fructose-induced adipose tissue insulin resistance through the insulin receptor substrate-1/phosphatidylinositol 3-kinase/Akt signaling pathway in rats, Toxicol. Appl. Pharmacol. 277 (2014) 155–163.

[50] X. Wang, R. Liu, W. Zhang, X. Zhang, N. Liao, Z. Wang, W. Li, X. Qin, C. Hai, Oleanolic acid improves hepatic insulin resistance via antioxidant, hypolipidemic and anti-inflammatory effects, Mol. Cell. Endocrinol. 376 (2013) 70–80.

[51] L. Shi, W. Zhang, Y.Y. Zhou, Y.N. Zhang, J.Y. Li, L.H. Hu, J. Li, Corosolic acid stimulates glucose uptake via enhancing insulin receptor phosphorylation, Eur. J. Pharmacol. 584 (2008) 21–29.

[52] K. Horiuchi, S. Shiota, T. Hatano, T. Yoshida, T. Kuroda, T. Tsuchiya, Antimicrobial activity of oleanolic acid from *Salvia officinalis* and related compounds on vancomycin-resistant enterococci (VRE), Biol. Pharm. Bull. 30 (2007) 1147–1149.

[53] G.P.P. Kamatou, S.F. Van Vuuren, F.R. Van Heerden, T. Seaman, A.M. Viljoen, Antibacterial and antimycobacterial activities of South African *Salvia* species and isolated compounds from *S. chamelaeagnea*, S. Afr. J. Bot. 73 (2007) 552–557.

[54] T.A. Ibrahim, Chemical composition and biological activity of extracts from *Salvia bicolor* Desf. growing in Egypt, Molecules 17 (2012) 11315–11334.

[55] A. Alrezaki, N. Aldawood, S. Alanazi, M. Arafah, Z. Fabova, Y. Badjah, A.V. Sirotkin, S. Alwasel, A. Halim Harrath, Consumption of sage (*Salvia offici-*

nalis) promotes ovarian function by stimulating estradiol hormone release and controlling folliculogenesis, steroidogenesis, and autophagy, J. King Saud Univ. Sci. 33 (2021) 101319.
[56] K. Ninomiya, H. Matsuda, H. Shimoda, N. Nishida, N. Kasajima, T. Yoshino, T. Morikawa, M. Yoshikawa, Carnosic acid, a new class of lipid absorption inhibitor from sage, Bioorg. Med. Chem. Lett. 14 (2004) 1943–1946.
[57] X. Li, S. Morita, H. Yamada, K. Koga, W. Ota, T. Furuta, A. Yamatsu, M. Kim, Free linoleic acid and oleic acid reduce fat digestion and absorption *in vivo* as potent pancreatic lipase inhibitors derived from sesame meal, Molecules 27 (2022) 4910.
[58] P. Mena, M. Cirlini, M. Tassotti, K.A. Herrlinger, C. Dall'Asta, D. Del Rio, Phytochemical profiling of flavonoids, phenolic acids, terpenoids, and volatile fraction of a rosemary (*Rosmarinus officinalis* L.) extract, Molecules 21 (2016) 1576.
[59] M.B. Hossain, D.K. Rai, N.P. Brunton, A.B. Martin-Diana, C. Barry-Ryan, Characterization of phenolic composition in Lamiaceae spices by LC-ESI-MS/MS, J. Agric. Food Chem. 58 (2010) 10576–10581.
[60] K. Miura, H. Kikuzaki, N. Nakatani, Apianane terpenoids from *Salvia officinalis*, Phytochemistry 58 (2001) 1171–1175.
[61] N.G.E.R. Etsassala, A.O. Adeloye, A.E. Halawany, A.A. Hussein, E.I. Iwuoha, Investigation of in-vitro antioxidant and electrochemical activities of isolated compounds from *Salvia chamelaeagnea* p.J. bergius extract, Antioxidants 8 (2019) 98.
[62] M. Tabefam, M.M. Farimani, O. Danton, J. Ramseyer, M. Kaiser, S.N. Ebrahimi, P. Salehi, H. Batooli, O. Potterat, M. Hamburger, Antiprotozoal diterpenes from *Perovskia abrotanoides*, Planta Med. 84 (2018) 913–919.
[63] J.G. Marrero, L. Moujir, L.S. Andrés, N.P. Montano, L. Araujo, J.G. Luis, Semisynthesis and biological evaluation of abietane-type diterpenes, revision of the structure of rosmaquinone, J. Nat. Prod. 72 (2009) 1385–1389.
[64] Z. Sadeghi, M. Masullo, A. Cerulli, F. Nazzaro, M.M. Farimani, S. Piacente, Terpenoid constituents of *Perovskia artemisioides* aerial parts with inhibitory effects on bacterial biofilm growth, J. Nat. Prod. 84 (2021) 26–36.
[65] P.C. Santos-Gomes, R.M. Seabra, P.B. Andrade, M. Fernandes-Ferreira, Phenolic antioxidant compounds produced by *in vitro* shoots of sage (*Salvia officinalis* L.), Plant Sci. 162 (2002) 981–987.
[66] E. Climati, F. Mastrogiovanni, M. Valeri, L. Salvini, C. Bonechi, N.Z. Mamadalieva, D. Egamberdieva, A.R. Taddei, A. Tiezzi, Methyl carnosate, an antibacterial diterpene isolated from *Salvia officinalis* leaves, Nat. Prod. Commun. 8 (2013) 429–430.
[67] M.B. Farhat, M.J. Jordán, R. Chaouch-Hamada, A. Landoulsi, J.A. Sotomayor, Changes in phenolic profiling and antioxidant capacity of *Salvia aegyptiaca* L. by-products during three phenological stages, LWT Food Sci. Technol. 1 (2015) 791–797.
[68] M.B. Farhat, J.A. Sotomayor, M.J. Jordán, Antioxidants of *Salvia aegyptiaca* L. residues depending on geographical origin, Biocatal. Agric. Biotechnol. 17 (2019) 486–491.
[69] M.B. Farhat, J.A. Sotomayor, M.J. Jordán, *Salvia verbenaca* L. essential oil: Variation of yield and composition according to collection site and phenophase, Biochem. Syst. Ecol. 82 (2019) 35–43.
[70] L. Pizzale, R. Bortolomeazzi, S. Vichi, E. Überegger, L.S. Conte, Antioxidant activity of sage (*Salvia officinalis* and *S. fruticosa*) and oregano (*Origanum onites* and *O. indercedens*) extracts related to their phenolic compound content, J. Sci. Food Agric. 82 (2002) 1645–1651.
[71] Y. Lu, L.Y. Foo, Antioxidant activities of polyphenols from sage (*Salvia officinalis*), Food Chem. 75 (2001) 197–202.
[72] M. Gantner, M. Brodowska, E.G. Horczyczak, I.W. Kalinowska, A. Najda, E. Pogorzelska, J. Godziszewska, Antioxidant effect of sage (*Salvia officinalis* L.) extract on turkey meatballs packed in cold modified atmosphere, CYTA J. Food 16 (2018) 628–636.
[73] M.F. Chaban, C. Karagianni, M.B. Joray, D. Toumpa, C. Sola, M.I. Crespo, S.M. Palacios, C.M. Athanassopoulos, M.C. Carpinella, Antibacterial effects of extracts obtained from plants of Argentina: Bioguided isolation of compounds from the anti-infectious medicinal plant *Lepechinia meyenii*, J. Ethnopharmacol. 239 (2019) 111930.
[74] C. Theoduloz, M.W. Pertino, J.A. Rodriguez, G. Schmeda-Hirschmann, Gastroprotective effect and cytotoxicity of carnosic acid derivatives, Planta Med. 77 (2011) 882–887.